Synthesis of Infinite-layered Superconductors under High Pressure

AUTHOR(S):

Azuma, Masaki; Ikeda, Nariaki; Hiroi, Zenji; Takano, Mikio; Bando, Yoshichika; Takeda, Yasuo

Bull. Inst. Chem. Res., Kyoto Univ., Vol. 70, No. 5-6, 1993

Synthesis of Infinite-layered Superconductors under High Pressure

Masaki AZUMA*, Nariaki IKEDA*, Zenji HIROI*, Mikio TAKANO*, Yoshichika BANDO*, and Yasuo TAKEDA**

Received December 18, 1992

High quality samples of both the alkaline earth-deficient type ($A_{1-x}CuO_{2-\delta}$, A: alkaline-earth element) and the rare earth-substituted type ($Sr_{1-x}R_xCuO_2$, R: rare-earth element) infinite-layered superconductors were synthesized using a cubic anvil high-pressure apparatus and were investigated physically and structurally. $A_{1-x}CuO_{2-\delta}$ contains defect layers where vacancies of both A cations and oxide ions concentrate. The superconducting properties change from *p*-type with the highest T_c of 110 K to *n*-type with $T_c \sim 40$ K via an insulative state depending on oxygen content. $Sr_{1-x}R_xCuO_2$, an *n*-type superconductor, does not change its T_c from 44 K depending upon either the kind or the concentration of dopant.

KEY WORDS: Infinite-layer structure/ Superconductivity/ Nonstoichiometry/ Microstructure

INTRODUCTION

Since 1986 many kinds of cupric oxide superconductors have been found. They all have such a common structural feature that negatively charged CuO_2 planes and positively charged counter layers are stacked alternately. The simplest structure containing CuO_2 planes is the so-called infinite-layer structure found in $ACuO_2$. As illustrated in Fig. 1 the CuO_2 planes are separated only by alkaline-earth ions in this structure. This has been considered as "the parent structure of cupric oxide superconductors", and after the first report concerning $Ca_{0.86}Sr_{0.14}CuO_2$ by Siegrist et al,[1] many efforts have been made to dope it with carriers and make it superconducting. At ambient pressure this structure is stable only for a narrow composition range around A $\sim Ca_{0.9}Sr_{0.1}$.[1,2] On the other hand, we found that application of high pressure effectively widened the composition range so that large A ions might be contained from A = $Ca_{2/3}Sr_{1/3}$ up to $Ba_{1/3}Sr_{2/3}$ through $SrCuO_2$.[3] More recently, we discovered a new superconductor crystallizing in a modified infinite-layer structure with the highest T_c of 110 K[4,5] by treating slightly A-deficient compositions under oxidizing atmosphere. The *p*-type character has thus been suggested. Moreover, we have found that superconductivity of probably *n*-type with $T_c \sim 40$ K can be obtained if the same starting material is treated under a reducing atmosphere. Besides, $Sr_{1-x}R_xCuO_2$ (R = Nd,

* 東 正樹, 池田成明, 広井善二, 高野幹夫, 坂東尚周: Laboratory of Solid State Chemistry II, Institute for Chemical Research, Kyoto University, Uji, Kyoto-fu 611, Japan
** 武田保雄: Department of Chemistry, Faculty of Engineering, Mie University, Tsu, Mie-ken 514, Japan

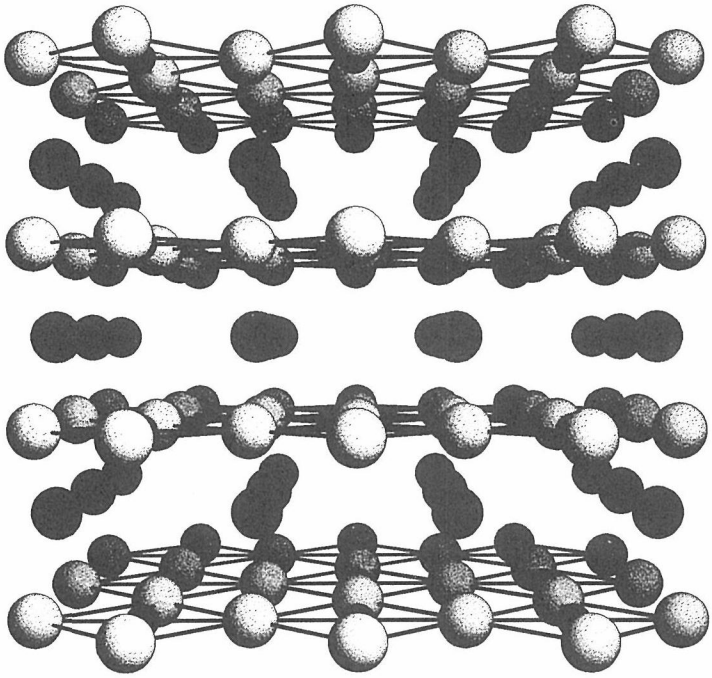

Fig. 1 Infinite-layer structure. Bright large spheres and dark large spheres are oxygen atoms and A atoms, respectively and small black spheres are copper atoms.

Pr[6], La[7]) crystallizing in the ideal, non-defect-featured structure have also been reported, where the substitution of trivalent R ions makes it *n*-type.

These infinite-layer phases would provide us with the most suitable stage to study high-T_c superconductivity because of the structural and compositional simplicity. However, the necessity to use high pressure has obstructed us in obtaining samples adequate for physical measurements in quality and quantity. In this paper, we report the synthesizing conditions to obtain high quality samples of both the A-deficient and the R-substituted types, and some physical and structural properties of these systems will be discussed.

EXPERIMENTAL

Samples were synthesized using a classical cubic anvil apparatus. Illustrated in Fig. 2 is the high pressure cell assemblage we used. A gold capsule charged with starting powder was inserted into a pyrophyllite cell together with a graphite heater, Mo electrodes and a Pt/Pt-13%Rh thermocouple. A BN sleeve was used as an insulator. The dimensions of the gold capsule was 3 mm $\phi \times$ 3 mm, limiting the sample weight to about 50 mg. The pellet was compressed and then heated for 0.5 ~ 2 h, and finally quenched to room temperature before releasing the pressure.

The atmosphere during the synthesis was controlled in the following four ways.

(1) Sample powder was enclosed in a gold capsule to make the inside atmosphere inert.

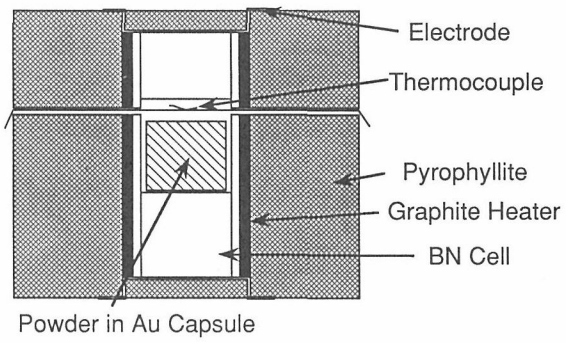

Fig. 2 High-Pressure cell assembly.

(2) $KClO_4$ was added to the bottom of the capsule to apply a high oxygen pressure. $KClO_4$ and the sample were separated from each other with a gold sheet.
(3) Ti powder was used instead of $KClO_4$ in order to generate a reducing atmosphere.
(4) Sample powder was packed directly in the BN sleeve: The surrounding graphite heater generated a strongly reducing atmosphere.

Applied pressure was 6 GPa for samples with A-deficient compositions, while it was 3 GPa for R-substituted samples. The temperature of heat treatment was varied depending mainly upon the atmosphere, being 1223 K for the oxidizing atmosphere, and 1173 K for the inert and the reducing atmospheres. Above these temperatures $A_4Cu_6O_{10}$,[8] an insulating layered material, was stablized so that monophasic infinite-layer compounds could not be obtained.

The starting oxides for A-deficient samples were prepared in the following three ways.
(a) $CaCO_3$, $SrCO_3$ and CuO mixed at ratios of $Sr/(Ca + Sr) = y$, $(Ca + Sr)/Cu = 1 - x$ were heated in an oxygen stream of ambient pressure at 1223 K. The product contained $ACuO_2$ (low-pressure phase) and $A_{14}Cu_{24}O_{41}$.
(b) $Ca_{1-y}Sr_yCuO_2$, the low-pressure phase synthesized in air at 1223 K, and CuO were mixed mechanically.
(c) $Ca_{1-y}Sr_yCuO_2$ prepared in an oxygen stream of ambient pressure at 1223 K and CuO were mixed mechanically.

For the R-substituted type samples intimate mixtures of $SrCuO_2$, R_2O_3 (R = La, Nd, Sm, Gd), and CuO were used as the starting materials.

The final products were characterized by powder X-ray diffraction (XRD) using CuKα radiation, electron diffraction (ED), and high-resolution electron microscopy (HREM). Magnetization was measured with a SQUID magnetometer (Quantum Design, MPMS2) in an external field of 10 Oe between 5 ~ 350 K. Resistivity was measured with a standard four terminal method.

RESULTS AND DISCUSSION

Synthesizing conditions and superconducting properties of alkaline earth-deficient type

Figure 3 shows the XRD patterns of $(Ca_{1-y}Sr_y)_{1-x}CuO_{2-\delta}$ with $x = 0$, 0.06 and $y =$

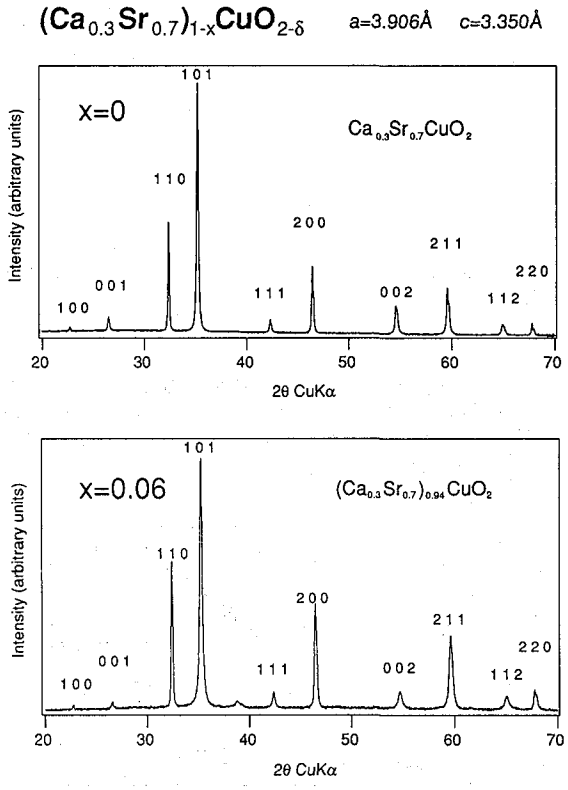

Fig. 3 X-ray diffraction patterns of $(Ca_{0.3}Sr_{0.7})_{1-x}CuO_{2-\delta}$ for x = 0 and 0.06. The indexing assumes an infinite-layer tetragonal unit-cell with a = 3.906Å and c = 3.353Å.

0.7 synthesized in the inert atmosphere from starting material (a). The peaks in both patterns can be indexed assuming an infinite-layer tetragonal unit-cell with a = 3.906 Å and c = 3.353Å. Peaks become broader with increasing A-cation deficiency for $x \leq 0.05$, while peaks due to CuO appear for $x \geq 0.05$. This result suggests that the infinite-layer structure can contain A-cation deficiency up to 5%.

When treated in either the oxidizing or reducing atmosphere, A-deficient compounds become superconducting. For these samples, starting material (b) or (c) was chosen, because $A_{14}Cu_{24}O_{41}$ coexisting in starting material (a) remained stable even at 6 GPa in the oxidizing atmosphere and survived in the final products. On the other hand, small amounts of CuO remained in samples prepared from mixtures (b) and (c) as shown in Fig. 4 because of the poor reactivity of these mechanical mixtures.

The temperature dependences of magnetic susceptibility (magnetization divided by applied field, M/H) and resistivity of $(Ca_{0.3}Sr_{0.7})_{0.9}CuO_{2-\delta}$ prepared in the oxidizing atmosphere from starting material (b) are shown in Fig. 5. A large diamagnetic signal with an onset temperature of 110 K is observed in the susceptibility curve. The second drop at 70 K does not seem to be due to weak coupling of local superconducting regions but seems to be due to the coexistence of another superconducting phase with a lower T_c, because the

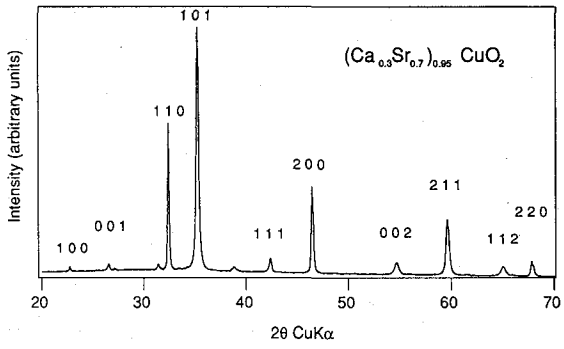

Fig. 4 X-ray diffraction pattern of $(Ca_{0.3}Sr_{0.7})_{0.95}CuO_{2-\delta}$ synthesized from starting material (c) in the oxidizing atmosphere. The weak peaks come from CuO and a compound of the $Sr_{14}Cu_{24}O_{41}$ type.

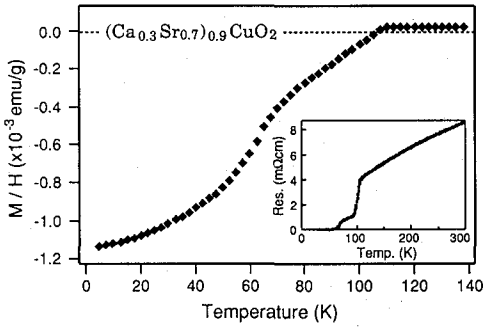

Fig. 5 Typical temperature dependences of magnetic susceptibility (M/H) measured for a powdered sample in an external field of 10 Oe on cooling and of resistivity of $(Ca_{0.3}Sr_{0.7})_{0.9}CuO_{2-\delta}$ synthesized in the oxidizing atmosphere from starting material (b).

drop survived at a high external magnetic field of 1000 Oe. A Meissner fraction of $\sim 10\%$ is estimated at 5 K, which is reasonably large for the fine particle size of $\leq 1\ \mu$m as measured by a scanning electron microscope. Resistivity shows metallic behavior and begins to drop at ~ 110 K in correspondence with the diamagnetism and becomes zero within experimental error at 50 K. The origin of the coexistence of the two superconducting phases with different T_c's has been attributed to an inhomogeneity in oxygen content. In support of this a subsequent annealing at 873 K before releasing the pressure or the use of starting material (c), which has proved to be more reactive, has been found to suppress the coexistence and give rise to a single sharp transition.

Figure 6 shows magnetic data for three samples of $(Ca_{0.3}Sr_{0.7})_{0.95}CuO_{2-\delta}$ synthesized from the same starting material (c) but compressed and heated in different atmospheres. The sample treated in the oxidizing atmosphere shows a sharp transition at 100 K and a large diamagnetic signal, while the one treated in the inert condition shows a weakly paramagnetic behavior at low temperature. On the other hand, the sample treated in the

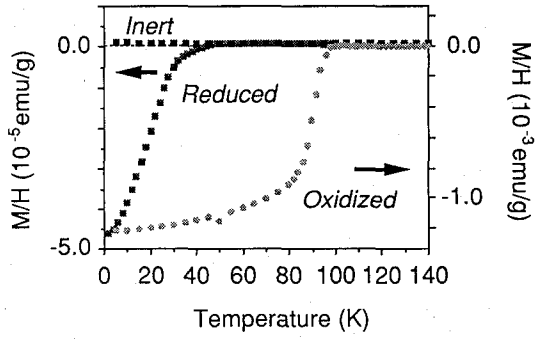

Fig. 6 Temperature dependences of magnetic susceptibility (M/H) measured in an external field of 10 Oe for three powdered samples of $(Ca_{0.3}Sr_{0.7})_{0.95}CuO_{2-\delta}$ synthesized from the same starting material (c) but in the oxidizing, inert, and reducing atmosphere.

strongly reducing atmosphere generated by the graphite heater shows a superconducting transition at $T_c \sim 40$ K, though its Meissner fraction is considerably smaller than that of the oxidized sample. The sample synthesized in the reducing atmosphere generated by Ti powder did not show any superconductivity probably because of the weak reducing force.

The results of chemical analysis for several samples by means of iodometry are collected in Table 1. The formal copper valence of the oxidized and reduced superconducting samples are about 2.1 and 1.9, respectively, strongly supporting the assertion that the former is p-type while the latter is n-type. In the insulating sample treated in the inert atmosphere , the formal copper valence is almost 2. The oxygen content calculated assuming the nominal metallic composition is nearly 2.0 for the oxidized sample, while it is less than 2 for those prepared in either the inert or the reducing condition, indicating oxygen deficiency in these two kinds.

Table 1 Copper valence determined by means of iodometry and oxygen content calculated assuming the nominal metallic composition.

No.	A deficiency	Condition	Cu valence	Oxygen
	x		$2+p$	$2-\delta$
142	0.1	inert	2.012	1.906
158	0.02	inert	1.999	1.980
157	0.02	Oxidized	2.179	2.069
163	0.05	Oxidized	2.113	2.009
188	0.05	Oxidized	2.116	2.008
222	0.1	Oxidized	2.117	1.958
123	0	Reduced	1.816	1.908
189	0.05	Reduced	1.902	1.901

Synthesizing conditions and superconducting properties of rare earth-substituted type

In previous reports, n-type superconductors, $Sr_{1-x}R_xCuO_2$, were synthesized under a reduced atmosphere generated by graphite.[6,7] According to our experience, however,

samples prepared in this way contained considerable amounts of impurity phases. Then, we enclosed a sample in a gold capsule with Ti powder working as an oxygen getter, and almost monophasic samples of $Sr_{1-x}R_xCuO_2$ were obtained as seen in the XRD pattern shown in Fig. 7. Experimental results concerning $Sr_{1-x}Nd_xCuO_2$ perpared in this way will be reported below.

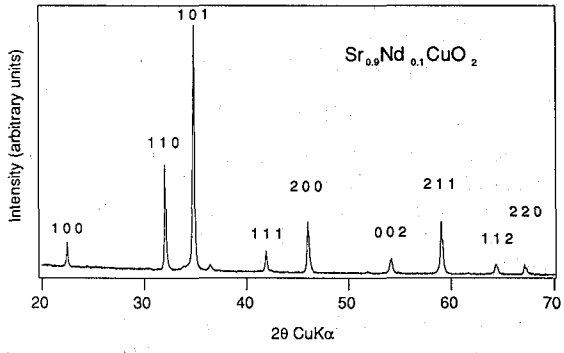

Fig. 7 X-ray diffraction pattern of $Sr_{0.9}Nd_{0.1}CuO_2$. The weak impurity peaks come from Cu_2O.

The lattice constants are plotted in Fig. 8. As Nd content increases, the *a*-axis increases its length, while the *c*-axis decreases its length. Below $x = 0.1$ both *a*- and *c*-axes change monotonically, but the changes seem to be saturated at $x = 0.1$. Above this Nd content impurity peaks appear, suggesting that the solubility limit is $x = 0.1$.

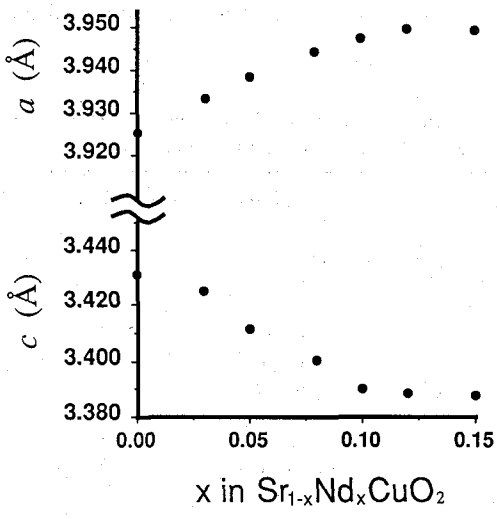

Fig. 8 Nd concentration dependence of the lattice constants for $Sr_{1-x}Nd_xCuO_2$. Both *a*- and *c*-axes are saturated at $x = 0.1$ indicating the solubility limit.

Iodometry revealed that oxygen content of monophasic samples is always 2, independent of the Nd concentration. It probably is the reason why this superconductor does not need such a strong reducing condition as generated by the surrounding hot graphite heater used for the preparation of the R-free but A- and oxygen-deficient superconductor mentioned previously.

Figure 9 shows the magnetic data for $Sr_{1-x}Nd_xCuO_2$. The Meissner fraction increases with increasing x, but T_c is 44 K for all samples. It is to be noted that neither their average structure studied by XRD nor their microscopic structure studied by ED and HREM are indicative of any phase separation. We thus suggest that an unavoidable statistical fluctuation in Nd content causes the coexistence of superconducting and non-superconducting regions. Moreover, substitution of La, Sm and Gd instead of Nd has been found not to change the T_c almost at all, and the value is very close to that of the reduced alkaline earth-deficient type, also. Details of the study in this system will be published elsewhere.[9)]

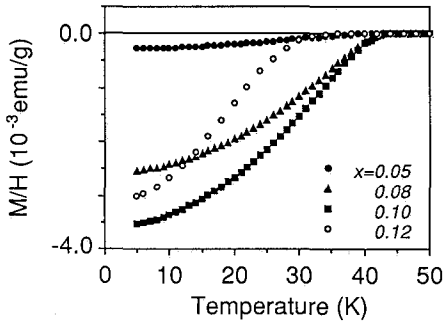

Fig. 9 Temperature dependences of magnetic susceptibility (M/H) in an external field of 10 Oe measured on cooling for $Sr_{1-x}Nd_xCuO_2$. The Meissner fraction increases with increasing x, while T_c is kept at 44 K.

Microstructure of alkaline-earth deficient infinite-layer phase

Previously we reported that the A-deficient infinite-layer phases prepared in the oxidizing and inert atmosphere involve "defect" layers inserted into the structure rather randomly.[5)] An essentially the same microstructure has been observed in the reduced samples as well. Figure 10 shows an electron micrograph of $(Ca_{0.3}Sr_{0.7})_{0.95}CuO_{2-\delta}$ treated in the reducing condition. It is a cross-sectional view of the layered structure, and the bright dot rows running horizontally (marked with arrows) correspond to the projections of defect-layers. They are inserted at intervals of 5 to a few ten times the c-axis in the image. The ED pattern in the inset reveals a streaking along the c^*-axis arising from the random distribution of the planar defects, and this is also the origin of the peak broadening in XRD patterns. However, the strong fundamental spots guarantee that the infinite-layered stacking is preserved throughout the crystal. The average defect-layer density seems to increase with increasing x.

In order to obtain further information on the mechanism of carrier doping, we performed a HREM observation of the defect-layers.[10)] Figure 11 shows a HREM image of

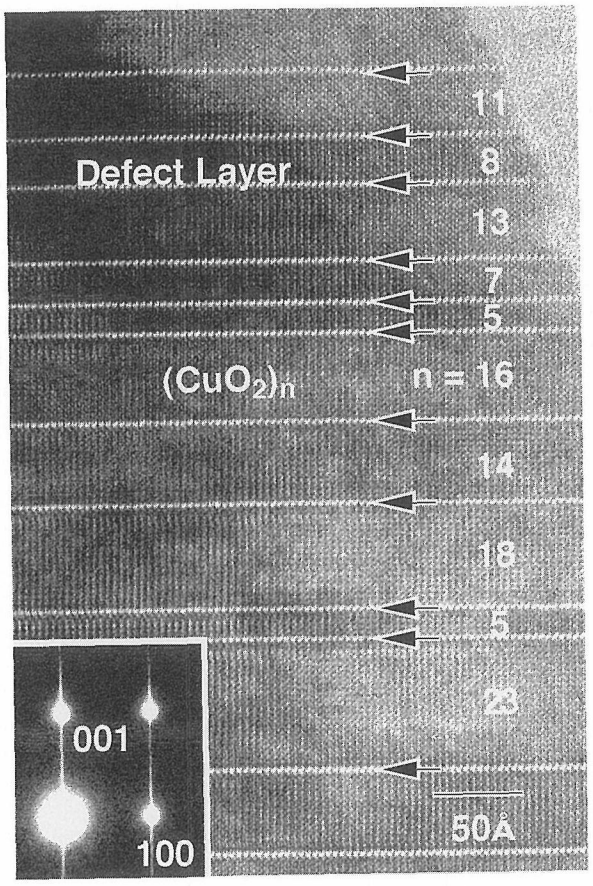

Fig. 10 HREM image and the corresponding ED pattern of $(Ca_{0.3}Sr_{0.7})_{0.95}CuO_{2-\delta}$ treated in the reducing condition. The defect-layers which appear as bright-dot rows are marked with arrows, and the numbers of CuO_2 sheets existing between two adjacent defect-layers are given in the image.

the defect-layers (marked with arrows again) found in the reduced sample. The incident electron beam is parallel to the *b* direction, giving a cross-sectional atomic view of the layer stacking. Since it was taken under a condition near the Scherzer defocus, a dark dot can be directly interpreted as an atomic column along the incident beam.

The following points are remarkable. Triple Cu-O sheets are involved in each defect layer and have an elongated intersheet distance of about 3.7Å, longer by 10% in comparison with the normal distance. The central Cu-O sheet in the defect layer contains a considerable amount of oxygen vacancies as seen from the much brighter contrast of the oxygen sites in this sheet than that in the other normal CuO_2 sheets. However, the brightness of the central Cu-O sheet is weak for oxidized samples as compared in Fig. 12. To make this point clear, the photodensity profiles along A-O atom lines (parallel to the *c*-axis), line P-Q for the oxidized sample and line R-S for the reduced sample, are plotted.

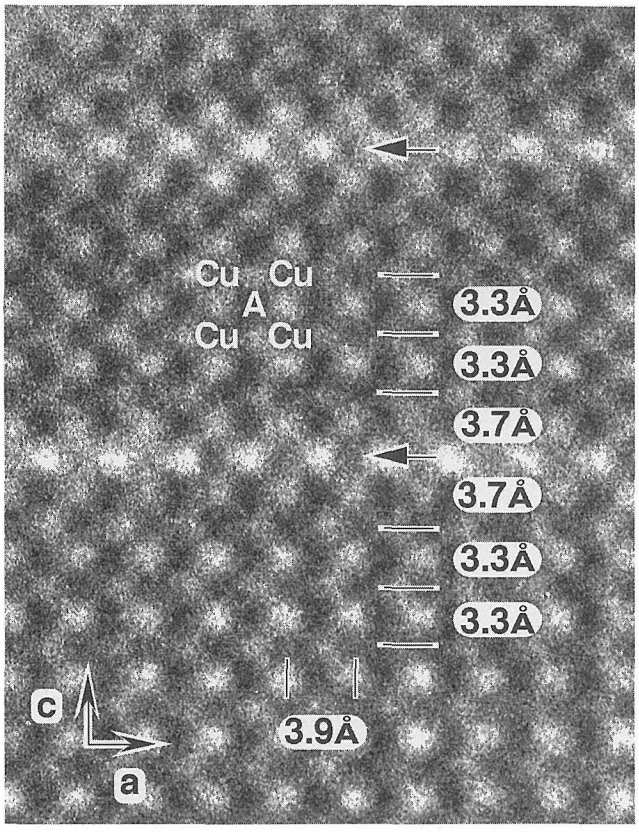

Fig. 11 HREM image of a defect-layers found in the reduced sample. Small and large dark dots correspond to Cu- and A-ions, respectively. The oxygen sites in the central Cu-O sheet of the defect-layer are much brighter than those of the normal CuO_2 sheet, suggesting the existence of a considerable amount of oxygen vacancies. The intersheet distance is elongated in the defect-layer.

The peaks in these profiles correspond to the oxygen sites and the valleys to the A sites. The oxygen site in the central Cu-O sheet is much brighter in the reduced sample than in the oxidized sample, indicating that the amount of oxygen vacancies is much larger in the former. The intersheet distance, however, does not vary remarkably with the atmosphere, which suggests that oxygen atoms are introduced only into the central sheet but not into the A-sheets located above and below it.

These results have provided us with such a structural image illustrated in Fig. 13. The structure is basically made of the infinite-layered stacking but includes defect-layers inserted rather randomly, in every several or a few tens of CuO_2 sheets. Each defect layer is formulated as $A_{1-z}/CuO_{2-\Delta}/A_{1-z}$ ($z > x$, $\Delta > \delta$). When treated in the inert atmosphere, oxygen vacancies in the central $CuO_{2-\Delta}$ sheet counteract the alkaline-earth vacancies ($\delta = x$), so that the copper valence is kept at 2+ and the sample remains insulating. In the oxidizing condition the oxygen vacancies are depleted ($\delta \sim 0$), and the sample be-

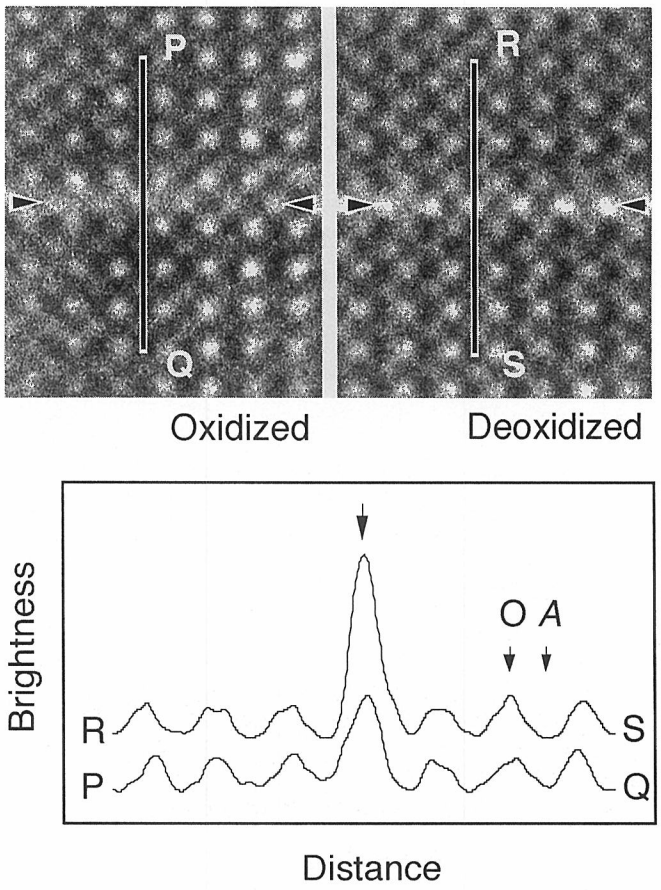

Fig. 12 Comparison of HREM images of the defect-layers obtained from an oxidized and a reduced samples. Photodensity profiles along the A-O atom lines, P-Q and R-S, are plotted, where the peaks correspond to the oxygen sites and the valleys to the A sites. The oxygen site for the central Cu-O sheet in the defect layer is much brighter in the reduced sample than in the oxidized sample, indicating that the amount of oxygen vacancies is much larger in the former.

comes a *p*-type superconductor with a $T_c \leq 110$ K. However, in the reducing condition oxygen vacancy content is further increased, inducing an *n*-type superconductivity with $T_c \sim 40$ K.

It is quite a remarkable, unique behavior of the A-deficient infinite-layer phase that it changes the sign of carrier from *p*-type to *n*-type through an insulating state depending on the oxygen content. A further study of this interesting system would surely throw a new light upon the still hidden superconducting mechanism.

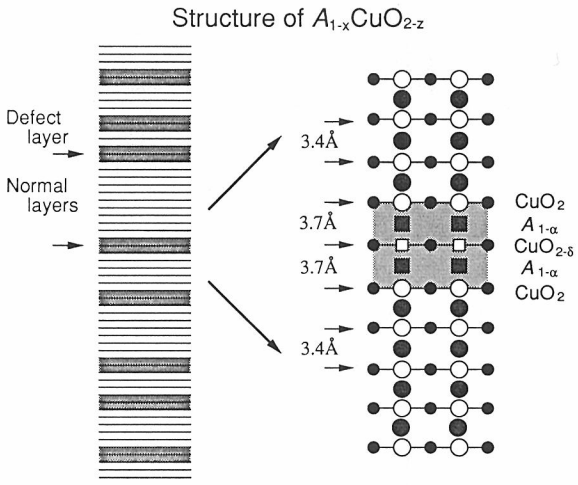

Fig. 13 Schematic representation of the structural characteristics of $A_{1-x}CuO_{2-\delta}$.

ACKNOWLEDGMENTS

The authors express their hearty thanks to O. Ohtaka, S. Kume and T. Yamanaka of Osaka University for permitting us to use their high pressure apparatus. This study was partly supported by a Priority-Areas Grant from the Ministry of Education, Science and Culture of Japan.

References

(1) T. Siegrist, S.M. Zahurac, D.W. Murphy, and R.S. Roth, *Nature,* **334**, 231 (1988).
(2) H. Yamane, Y. Miyazaki, and T. Hirai, *J. Cer. Soc. Jpn.,* **97**, 143 (1989).
(3) M. Takano, Y. Takeda, H. Okada, M. Miyamoto, and K. Kusaka, *Physica,* **C 159**, 375 (1989).
(4) M. Takano, M. Azuma, Z. Hiroi, Y. Bando, and Y. Takeda, *Physica,* **C 176**, 441 (1991).
(5) M. Azuma, Z. Hiroi, M. Takano, Y. Bando, and Y. Takeda, *Nature,* **356**, 775 (1992).
(6) M.G. Smith, A, Manthiran, J. Zhou, J.B. Goodenough and J.T. Markert, *Nature,* **351**, 549 (1991).
(7) G.Er,Y. Miyamoto, F. Kanamaru, and S. Kikkawa, *Physica,* **C 174**, 280 (1991).
(8) Z. Hiroi, M. Azuma, M. Takano, and Y. Bando, *J. Solid State Chem.,* **95**, 230 (1991).
(9) N. Ikeda, A. Hiroi, M. Azuma, M. Takano, and Y. Takeda, in praparation.
(10) Z. Hiroi, M. Azuma, M. Takano, and Y. Takeda, *Physica,* **C** in print.